Discussion of the Results

Solutions of Eq. (18) allow a description of the disturbances arising in a weakly ionized gas containing heat sources in the presence of an applied normal magnetic field. These solutions can be compared with those obtained by Glushkov and Kareev[2] for a neutral gas.

As before, the condition for generating disturbances in the gas can be written as

$$\left(\frac{\partial q_c}{\partial p}\right)_\rho < \frac{\kappa_s a_s}{\gamma - 1}\xi_c^* > 0 \qquad (23)$$

where ξ_c^* is determined from (19) and (20).

Notice that, although ξ_{cnp}^* does not change whether or not there is an applied $\boldsymbol{B}$ field, this is not the case for ξ_{cp}^* (Fig. 1). Actually, there exists a shift toward greater values of ξ_c if an ionized gas with an applied normal $\boldsymbol{B}$ field is considered. As shown by Glushkov and Kareev,[2] if condition (23) is met, fluctuations in the strength of heat sources can lead to both wave and aperiodic disturbances. However, one can see that the presence of the magnetic field causes a reduction in the values of $|y_i|$ for the same ξ_c.

As the criterion for absolute stability still is given by the aperiodic stability limit, which is almost insensitive to the $\boldsymbol{B}$ field, one may conclude that the characteristic dimension of an absolutely stable system again can be determined by the relationship suggested by Glushkov and Kareev.[2]

References

[1] Strutt, J. W. (Lord Rayleigh), *The Theory of Sound*, Dover, New York, 1945.

[2] Glushkov, I. S. and Kareev, Yu, A., *High Temperature*, Vol. 8, 1970, pp. 901-906.

[3] Sutton, G. W. and Sherman, A., *Engineering Magnetohydrodynamics*, McGraw-Hill, New York, 1956.

Light Reflection as a Simple Experimental Method in Compressible Boundary-Layer Studies

M. E. H. van Dongen*

Eindhoven University of Technology, Eindhoven, The Netherlands

Introduction

IN compressible flow investigations optical methods are extensively applied and offer a wide variety of possibilities. This paper discusses the application of light reflection as an experimental method to measure the local refractive index of a gas at the interface with a wall, even if rather strong gradients in temperature, density, or chemical composition of the gas exist. Such a situation is met in a compressible boundary layer adjacent to a wall. Let us assume that the wall is optically transparent and that a plane light wave is reflecting from the interface between wall and gas and from the boundary layer. It will be shown that if the ratio of the boundary layer thickness to the wavelength is not too small the reflections from the boundary layer itself vanish, and the refractive index of the gas at the wall is obtained by a measurement of the reflectivity.

Received Dec. 13, 1976; revision received April 22, 1977.

Index categories: Research Facilities and Instrumentation; Experimental Methods of Diagnostics.

*Research Scientist, Physics Department.

The refractive index of a gas depends on its density and chemical composition. Possible fields of application of the method are, therefore, mixing and diffusion processes, temperature jump, and chemical reaction phenomena in compressible boundary layers. Some applications of the method to the viscous side-wall and the thermal end-wall boundary layer in a shock tube are briefly discussed.

Theory

Consider a gaseous compressible boundary layer adjacent to an optically transparent wall. A plane light wave, linearly polarized, reflects partly from the plane of separation between the two media, partly from the gaseous inhomogeneity as indicated in Fig. 1. Subscript a will be used for the solid, s to indicate the gas state at $x=0$. The gas refractive index varies from a value n_s at the wall to n_∞ as $x \to \infty$. The angle between the direction of light propagation and the x direction is denoted by θ. A detailed discussion on light reflection from stratified media has been given by Jacobsson.[1]

We have to distinguish two different reflection phenomena, the direct reflection from the discontinuity and internal reflections from the boundary layer.

Direct Reflection from Discontinuity

The amplitude reflection coefficient for the direct reflection is given by

$$r_l = (\beta_s - \beta_a)/(\beta_s + \beta_a) \qquad (1)$$

with $\beta = n^2/(n^2-\alpha^2)^{1/2}$ for polarization parallel (‖), and with $\beta = (n^2-\alpha^2)^{-1/2}$ for polarization perpendicular ($\perp$) to the plane of incidence, respectively. Snell's invariant α is defined by $\alpha = n\sin\theta$. According to Eq. (1), r_l depends on n_s with α as a parameter that can be adjusted by varying the angle of incidence. In a gaseous medium the variation of n_s can be assumed to be very small with respect to unity. Therefore the relation between the reflectivity r_l^2 and n_s can be linearized in good approximation. We linearize r_l^2 with respect to its value for a uniform reference state, indicated by subscript 0

$$r_l^2 = r_{l0}^2(1 + S_l\Delta n) \qquad (2)$$

with $\Delta n = n_s - n_0$. The sensitivity S_l is defined as follows:

$$S_l = \frac{2}{r_{l0}}\left(\frac{\mathrm{d}r_l}{\mathrm{d}n_s}\right)_0 = \frac{4\beta_a}{\beta_0^2 - \beta_a^2}\left(\frac{\mathrm{d}\beta}{\mathrm{d}n}\right)_0 \qquad (3)$$

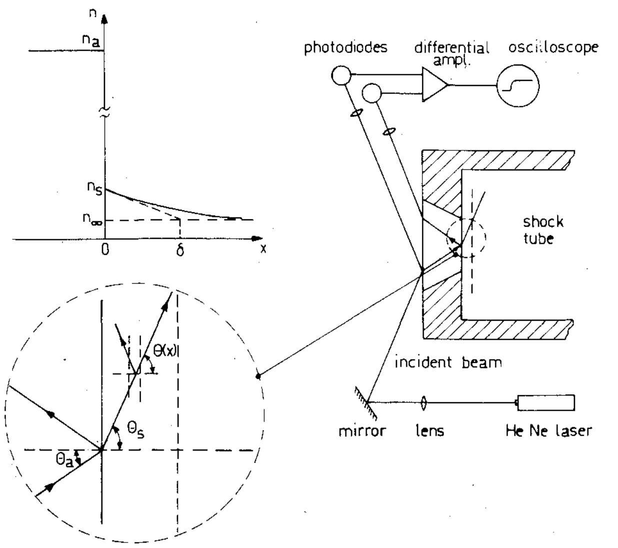

Fig. 1 Schematic representation of the refractive index profiles, the light wave trajectory, and the experimental setup.

A substitution of the definitions of β into Eq. (3) yields for S_l

$$(\parallel):\ S_l = -4\left(\frac{n_a^2-\alpha^2}{n_0^2-\alpha^2}\right)^{1/2} \times \frac{n_0 n_a^2(2\alpha^2-n_0^2)}{(n_a^2-n_0^2)(\alpha^2 n_a^2+\alpha^2 n_0^2-n_a^2 n_0^2)} \tag{4}$$

$$(\perp):\ S_l = -4\left(\frac{n_a^2-\alpha^2}{n_0^2-\alpha^2}\right)^{1/2} \frac{n_0}{n_a^2-n_0^2} \tag{5}$$

From Eqs. (4) and (5) it is found that the case of parallel polarization is more sensitive for refractive index variations than that of perpendicular polarization. The linearization procedure does not hold for α values close to $2^{-1/2} n_0$, and the Brewster value for parallel polarization and close to grazing incidence, $\alpha = n_0$.

Contribution of Internal Reflections

Each part of the boundary layer contributes to the net reflection coefficient. Neglecting multiple reflections and attenuation, the ratio of the wave amplitudes reflecting from and incident to the boundary layer is given by[1]

$$r_2 = \int_0^\infty \frac{1}{2\beta}\frac{d\beta}{dx} \exp\left[2ik\int_0^x n(x')\cos\theta(x')\,dx'\right] dx \tag{6}$$

where k denotes the wave number.

This expression can be understood as follows: each slab dx has a contribution $d\beta/2\beta$ to the reflection coefficient. The phase factor corresponds to twice the optical path difference between the reflecting plane and the origin. The angle $\theta(x')$ is related to $n(x')$ by Snell's law. Equation (6) can be simplified under the assumption that $\Delta n << 1$. We linearize $\beta(n)$ with respect to n_0 and approximate the phase factor by a linear relation in x:

$$r_2 = \Delta n \frac{1}{2\beta_0}\left(\frac{\partial\beta}{\partial n}\right)_0 \int_0^\infty F'(\hat{x})\exp(i\Omega\hat{x})\,d\hat{x} + O(\Delta n)^2 \tag{7}$$

with

$$\Omega = 2k\delta\langle n\cos\theta\rangle;\quad \hat{x}=x/\delta;\quad F=n(\hat{x})/\Delta n;\quad F'=dF/d\hat{x}$$

Direct and internal reflections have to be combined by the following combination rule,

$$r = (r_1+r_2)/(1+r_1 r_2) \tag{8}$$

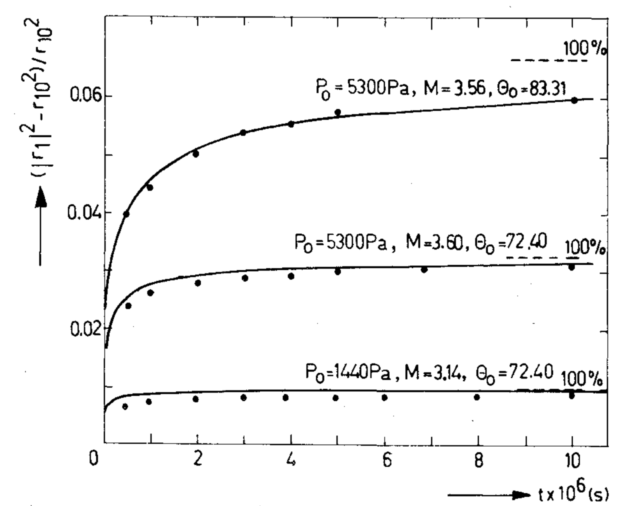

Fig. 2 Relative variation of reflectivity as a function of time for shock reflection in argon. ——theory; • experiment. The theoretical asymptotic values as $t \to \infty$ are indicated by: -----100%.

For any given refractive index profile, r can be calculated by combining Eqs. (1), (6) or (7), and (8).

Condition for Vanishing Internal Reflections

The contribution of the internal reflection depends on the boundary layer thickness δ. This can be investigated in more detail by expanding the expression of Eq. (7) for r_2 in an asymptotic series by repeated integration by parts

$$r_2 = \Delta n\frac{1}{2\beta_0}\left(\frac{\partial\beta}{\partial n}\right)_0 \left\{ i\frac{F'(0)}{\Omega} - \frac{F''(0)}{\Omega^2} - i\frac{F'''(0)}{\Omega^3} + \frac{F^{(4)}(0)}{\Omega^4} + \ldots \right\} \quad \text{as } \Omega\to\infty \tag{9}$$

A substitution of Eqs. (9) and (2) into Eq. (8) yields after some algebra,

$$\frac{|r|^2 - r_{10}^2}{r_{10}^2} = S_l(n_s-n_0)\left\{1 - \frac{F''(0)}{\Omega^2} + \frac{F^{(4)}(0)}{\Omega^4}\ldots\right\} + O(\Delta n)^2 \tag{10}$$

A general criterion for vanishing internal reflections cannot be given because Eq. (10) is an asymptotic series, not necessarily a convergent one. Calculations made with realistic boundary layer profiles showed that for $\Omega > 10$ the contribution of the internal reflections was indeed less than 1% as suggested by Eq. (10). In terms of the wavelength λ this would imply that $\delta/\lambda > 5/(2\pi\cos\theta_0)$. If this rather weak condition is fulfilled, a simple linear relation remains between the variation of the reflectivity and the variation of the gas refractive index at the wall:

$$\frac{|r^2| - r_{10}^2}{r_{10}^2} = S_l(n_s-n_0) \tag{11}$$

Shock Tube Applications

Thermal End-Wall Boundary Layer

When a shock wave reflects from the end wall of a shock tube, gas temperature and pressure change abruptly from their initial values T_0, p_0 to their higher reflected shock values T_∞, p_∞. Because the wall temperature itself changes only slightly, a thermal boundary layer is formed adjacent to the wall.[2] Its structure is approximately a function of $x/t^{1/2}$. Therefore the change in refractive index in the vicinity of the wall can be described by $n = n_0 + (n_s-n_0)H(t)G(x/t^{1/2})$,

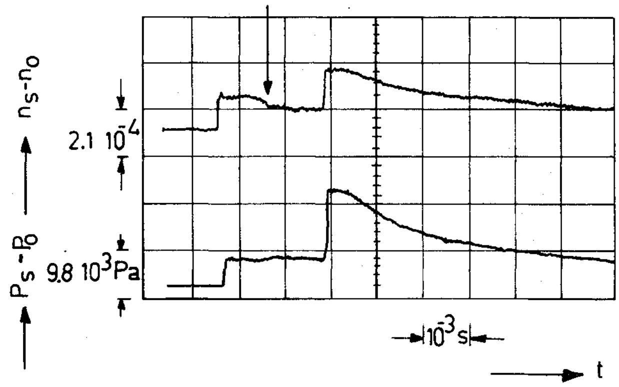

Fig. 3 Reproduction of an oscilloscope recording of the refractive index (upper curve) and the pressure (lower curve) at the side-wall of a shock tube. Test gas is nitrogen and driver gas is hydrogen; initial pressure = 2660 Pa, shock Mach number = 4.22.

$H(t)$ being the unit step function, while G represents the normalized boundary layer structure. This type of boundary layer is very suitable to check the present method experimentally and to investigate the effect of the internal reflections. The experimental setup is sketched in Fig. 1. The plane of polarization of the helium-neon laser beam is chosen parallel to the plane of incidence. The light beam reflecting from the outer surface of the shock tube window is used as a reference to reduce the effect of laser instabilities. The electronic circuit has a rise time less than 2.10^{-7} sec. In Fig. 2 some experimental and theoretical results are shown for the case of shock reflection in argon for different shock Mach numbers M, initial pressures p_0, and angles of incidence θ_0. Initially, the jump in direct reflection is compensated completely by the internal reflections inside the infinitely thin boundary layer. As the boundary layer grows, the internal reflections vanish and asymptotically a change in reflectivity is observed proportional to $(n_s - n_0)$. The solid curves show the theoretical predictions based on the substitution of a somewhat simplified boundary layer solution into Eqs. (1, 6, and 8).

The agreement is very satisfactory. The systematic deviation between theory and experiment for the lowest pressure is due to the phenomenon of temperature jump between gas and wall.

It is concluded from these experiments that the change in refractive index $(n_s - n_0)$ can be derived from the final change in reflectivity when the boundary layer thickness has become sufficiently large. This has been applied to study the influence of thermal diffusion in a thermal boundary layer in a mixture of argon and helium.[3] A separation of species could be shown by a measurement of the refractive index at the wall.

Viscous Side-Wall Boundary Layer

As a last example, we will discuss an application to the sidewall of a shock tube. At the passage of a shock wave the refractive index at the wall undergoes a jump proportional to the change in pressure. After some time the contact region will pass, separating driver and test gas.

Figure 3 shows the reproduction of an oscilloscope recording for an experiment with nitrogen as test gas and hydrogen as driver. The upper curve is obtained from the change in reflectivity, which is now proportional to $(n_s - n_0)$ since internal reflections can be completely neglected. The lower curve shows the pressure, measured with a piezoelectric transducer. The arrow indicates the arrival of the contact region, when the reflectivity signal starts decreasing due to the lower refractive index of hydrogen compared with nitrogen. After the passage of the reflected shock wave in hydrogen, expansion waves cause a decay in refractive index and in pressure. The experiment illustrates that the reflectivity method offers the possibility of distinguishing between different gases and can provide additional information on the state of a gas at a wall.

Acknowledgment

The author is indebted to J.F.H. Willems, H.J. Jager, and L.J.M. Haffmans for their experimental contributions.

References

[1] Jacobsson, R., "Light Reflection from Films of Continuously Varying Refractive Index," *Progress in Optics,* Vol. 5, North Holland Publishing Cie., Amsterdam, 1966, pp. 249-286.

[2] Clarke, J.F., "The Reflexion of a Plane Shock Wave from a Heat Conducting Wall," *Proceedings of the Royal Society,* A, Vol. 299, 1967, pp. 221-237.

[3] van Dongen, M.E.H., van Gils, J.F.M., Willems, J.F.H., and Vossers, G., "Thermal Diffusion in the End Wall Thermal Boundary Layer of a Shock Tube," *Proceedings of the Xth International Shock Tube Symposium,* Shock Tube Research Society, Japan, 1975, pp. 119-126.

Low Reynolds Number Flow Past a Blunt Axisymmetric Body at Angle of Attack

Ajay Kumar*
NASA Langley Research Center, Hampton, Va.

Nomenclature

C_D = total drag coefficient based on the local base area
C_{D_p} = pressure drag coefficient based on the local base area
c_f = skin-friction coefficient
c_H = heat-transfer coefficient, $\dot{q}'_w / \frac{1}{2}\rho'_\infty V'^3_\infty$
h = specific enthalpy, h'/V'^2_∞
n = normal coordinate, n'/R'_N
p = pressure, $p'/\rho'_\infty V'^2_\infty$
r = local body radius, r'/R'_N
R'_N = nose radius
Re = freestream Reynolds number, $\rho'_\infty V'_\infty R'_N / \mu'_\infty$
s = tangential coordinate, s'/R'_N
u = tangential velocity, u'/V'_∞
U_s = shock speed, U'_s / V'_∞
v = normal velocity component, v'/V'_∞
V'_∞ = freestream velocity
V_{N_∞} = freestream velocity normal to the shock, V'_{N_∞}/V'_∞
V_{T_∞} = freestream velocity tangential to the shock, V'_{T_∞}/V'_∞
ρ = density, ρ'/ρ'_∞
μ = viscosity, μ'/μ'_∞
γ = ratio of specific heats
α = angle of attack

Subscripts

N = conditions behind the shock
w = conditions at the body surface
∞ = conditions in the freestream

Superscript

$'$ = dimensional quantities

Introduction

THE problem of computing the laminar hypersonic flow at low Reynolds numbers past blunt axisymmetric bodies has been investigated by many authors[1-3] using viscous shock-layer equations or full Navier-Stokes equations; however, these investigations are limited to zero angle of attack. The purpose of this Note is to investigate the low Reynolds number flow of a perfect gas over a blunt axisymmetric body of large half-angle at small angles of attack, which represents the conditions encountered by the planetary entry probes during the early (high-altitude) portions of an atmospheric entry trajectory. Time-dependent viscous shock-layer equations are used to describe the flowfield. These equations are obtained from the full Navier-Stokes equations by keeping terms up to second order in the inverse square root of Reynolds number in both the viscous and inviscid regions. The equations are valid for moderate to high Reynolds numbers. A time asymptotic finite-difference method is used to solve these equations in the plane of symmetry of the flowfield. Since the crossflow velocity is identically zero in the plane of symmetry, the crossflow momentum equation cannot be used directly. The required equation is obtained by dif-

Received March 24, 1977.
Index categories: Viscous Nonboundary-Layer Flows; Supersonic and Hypersonic Flow.

*Postdoctoral Research Associate, National Research Council, Washington, D.C., working in the Computational Fluid Dynamics Group, Aerothermodynamics Branch, Space Systems Division. Member AIAA.